Frequency Domain Finite Element Approximations for Saturable Electrical Machines under Harmonic Driving Conditions

Johan Driesen and Kay Hameyer

Katholieke Universiteit Leuven, Dep. EE (ESAT), Div. ELEN
Kardinaal Mercierlaan 94, B-3001 Leuven, BELGIUM
e-mail : johan.driesen@esat.kuleuven.ac.be

Abstract

Electromagnetic devices are often operated under non-linear conditions. Therefore, the current and/or the voltage may not be sinusoidal. This is the case when power electronic sources or loads are applied. Ferromagnetic saturation causes the machine to behave non-linear as well. Four different FEM algorithms to simulate and approximate the joint effect of the mentioned combined non-linearities are discussed here. A practical example is used to illustrate and compare the approaches used.

Introduction

Saturated electromagnetic devices, such as saturated transformers and *AC*-machines, are more and more operated by power electronic converters. The machines are subject to non-sinusoidal voltage and current waveforms. Generator loads, such as photovoltaic inverters, are often non-linear. On the other hand, more and more electrical loads have to be considered severely non-linear as well. This behaviour is mainly caused by power electronic devices inside the loads with the associated control techniques.

Traditionally saturation effects are considered as only non-linear phenomena. This gave rise to quasi-static methods and algorithms using single harmonic models and equivalent material properties [1] that prove to work well for many types of machines in "traditional" periodic operating modes [2]. For "non-traditional" states, time-stepping approaches were advisable, yielding entire transient numerical models. However, often simplifying approximations can be found enabling to calculate many conditions by using less time consuming methods. Since the steady state is an important calculation aim, the frequency domain with its implicit assumption of a steady state condition, is a good mathematical solution domain to look for approximations.

FEM Approximations in the Frequency Domain

To describe the magnetic field in the frequency domain, the 2D vector potential equation is, before applying the FEM-method, transformed into the frequency domain (Fourier Transform):

$$\nabla \cdot \left(\mathrm{F}\{\upsilon(t)\} * \nabla\, \mathrm{F}\{A(t)\} \right) - \sigma\, \frac{\partial \mathrm{F}\{A(t)\}}{\partial t} = -\,\mathrm{F}\{J_s(t)\} \tag{1}$$

$$\text{with } B(t) = \nabla \times A(t) \tag{2}$$

The convolution product enables mathematically the generation of new frequencies. The time-derivative will be replaced by appropriate $j\omega$-operators. The Fourier spectra of the periodic fields are in fact discrete series. It is important that the frequency components are known in advance to be able to take advantage of the approximate methods. If the frequencies are unknown, time domain approximations can be applied.

Depending on the particular application and on the relative magnitude of the frequency components, different approximations can be performed, yielding non-linear computation algorithms with a varying degree of complexity.

Single harmonic approximation (time harmonic, sinusoidal)

In this time harmonic approach, only the fundamental magnetic field frequency component, modelled as a complex number and a *DC*-component of the (effective) reluctivity are considered [1,2]. It is possible to include

iron losses by using a complex reluctivity [3]. This can be considered as an elliptic approximation of the magnetic *BH*-characteristic. These assumptions yield:

$$\nabla \cdot \left(\underline{\upsilon}_{eq}(\underline{A})\nabla \underline{A}\right) - \sigma j\omega \underline{A} = -\underline{J}_{s,eq} \tag{3}$$

Multi-harmonic I

In the case the magnetic field contains a dominant fundamental frequency component, it can be assumed that the *DC*-saturation level is dominated by this component. A typical example of this situation is a magnetic device connected to a strong sinusoidal power grid feeding a non-linear load producing current harmonics. The total magnetic field can then be calculated by means of an uncoupled set of equations, with the harmonic equation (4) describing the dominant harmonic being the only non-linear equation and (5) determining the harmonic field components.

$$\nabla \cdot \left(\underline{\upsilon}_{eq}(\underline{A_1})\nabla \underline{A_1}\right) - \sigma j\omega \underline{A_1} = -\underline{J}_{s,1} \tag{4}$$

$$\nabla \cdot \left(\underline{\upsilon}_{eq}(\underline{A_1})\nabla \underline{A_h}\right) - \sigma j\omega_h \underline{A_h} = -\underline{J}_{s,h}, \, h>1 \tag{5}$$

Eq. (4) must be solved first, followed by the other field harmonics (eq. (5)). The solution of the harmonic fields can be parallelized because the saturation level is determined by the fundamental frequency (4).

Multi-harmonic II

In many cases, however, the field harmonics are important, e.g. when the supply voltage is non-sinusoidal and contains higher harmonics and the device is not too much saturated. Thus, all of the harmonics have to be considered to obtain the *DC*-saturation, but it is assumed that the field components do not mutually interact directly. Therefore, all the equations are non-linearly coupled.

$$\nabla \cdot \left(\underline{\upsilon}_{eq}\left(\{A_h\}_{h\geq 1}\right)\nabla \underline{A_h}\right) - \sigma j\omega_h \underline{A_h} = -\underline{J}_{s,h}, \, h\geq 1 \tag{6}$$

The different equations (6) are solved for a certain operating point, in which the saturation state is temporarily frozen. Hence, the set of equations becomes locally decoupled and can be calculated in parallel. The synchronisation point in this algorithm is the non-linear update of the material properties.

Harmonic Balance

When the mutual interactions between the different harmonics, expressed by the convolution product terms in eq. (1), caused by saturation, are modelled, the different equations become intensely coupled [4,5] and a full harmonic balance is required. Both, harmonics in the field as well as in the material series are included. FFT algorithms can be used to calculate this non-linear reluctivity updates.

$$\nabla \cdot \left(\sum_{i=-N}^{N} \upsilon_{h-i}\nabla A_i\right) - j\omega_h \sigma A_h = J_{s,h} \tag{7}$$

The semi-uncoupled multi-harmonic algorithms I and II have the advantage that they can be implemented in a parallel environment, such as a cluster of workstations. However, the harmonic balance algorithm can be parallelised up to a certain point, but in general more than one iteration over the different harmonic equations is required before a non-linear reluctivity update can be performed [5]. The very time consuming alternative is a sequential time-stepping non-linear simulation, accounting for all non-linearities.

Applications

For comparison, the discussed algorithms are applied to a single-phase transformer FEM model. The mesh is shown in Fig. 1. The core consists of ferromagnetic material. The discussed algorithms are implemented in an FEM package and parallelized using the PVM-library [5]. Hysteresis efects are neglected. Therefore, only odd harmonics are found in the magnetic field and the material series in the harmonic balance algorithm contains a *DC*-term and even harmonics only.
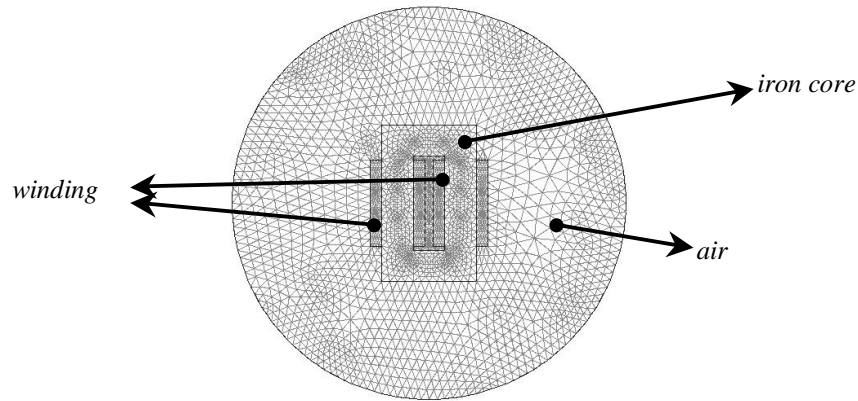
Fig. 1 2D-mesh of the transformer model used in calculations.

No-load condition with sinusoidal voltage

When the transformer is connected to a sinusoidal primary voltage of 300 V at 50 Hz, saturation of the magnetic material occurs in the corners of the yoke (Fig. 2). The adaptively refined mesh is refined in these locations. Only harmonics caused by saturation are found. Obviously, these do only occur in the multi-harmonic algorithms. The right-hand sides of the equations are filled in with the voltage source. At higher harmonic frequencies, the amplitude of these sources is zero. Saturation harmonics are found in the no-load current.

The solutions of the multi-harmonic algorithms I and II converge towards the single harmonic algorithm. Therefore only the harmonic balance is meaningful, since the off-diagonal convolution terms can be identified as arbitrary currents generating an – only mathematically meaningful – magnetic field. The first three solutions of the harmonic balance algorithm, performed on a series running up to the 15th field harmonic, are shown in Fig. 2. The 'arbitrary currents' in the corner indicate local saturation; they seem to push the flux out of the corners.

a) fundamental frequency   b) 3rd harmonic   c) 5th harmonic
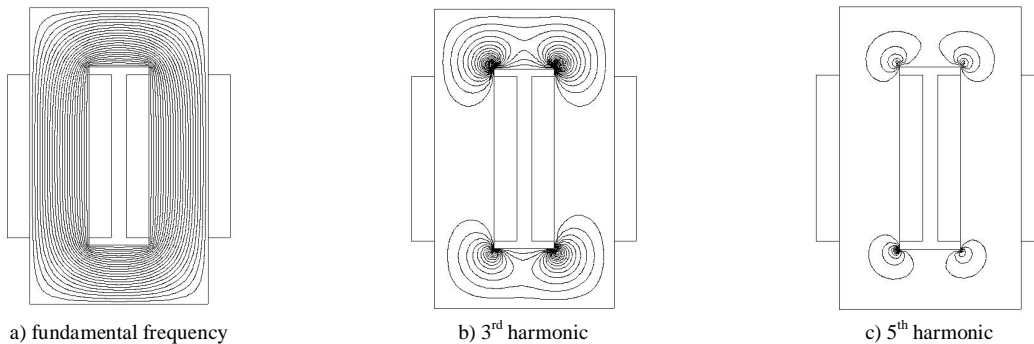
Fig. 2   Set of solutions by the harmonic balance algorithm on the single-phase transformer model.

No-load condition with square-wave voltage

In a second application, the same transformer is operated by a square-wave voltage. In this case the multi-harmonic I and II algorithms are useful and are forming an approximation to the exact solution. Fig. 3 shows the driving square-wave voltage for a low frequency approximation (see [5] for discussion), cutting off at 750 Hz.
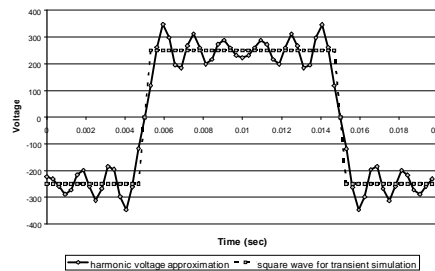

Fig. 3 Square wave approximation using a limited number of harmonics.

The difference between the algorithms can be noticed in a graph of the no-load currents (Fig. 4), with the exact current as obtained by a transient simulation for comparison. It can be seen that the harmonic balance algorithm follows the no-load current very good, until the sharp peak. At this point of strong ferromagnetic saturation, the frequencies are too high and are not considered in this approach. Here, multi-harmonic II overestimates the current, whereas the faster converging multi harmonic I comes close to the harmonic balance solution.
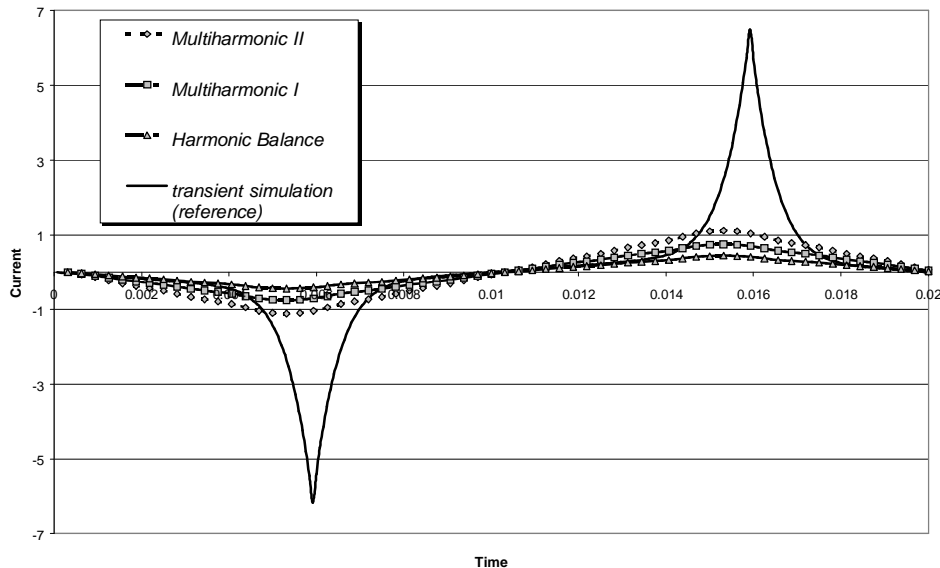

Fig. 4 No-load current under semi-square wave voltage compared for the different algorithms.

When (harmonic) loads are considered, identical results are obtained. Convergence is usually reached faster since the load-related harmonic leakage fluxes determine the high frequency fields.

Discussion and conclusion

In general MH II seems to overestimate the saturation effects more than MH I, since it averages them out over the whole time span. MH I works fine when there is a dominant fundamental as it is the case with most PWM-schemes. Harmonic balance can account for the time-local occurrence of saturation up till a preset maximum frequency and delivers the best approximation, but leads to longer computation times and a more difficult convergence behaviour.

Acknowledgement

References

[1] E. Vassent, G. Meunier, J.C. Sabonnadière, "Simulation of induction machine operation using complex magnetodynamic finite elements," IEEE Trans. on Magn., vol. 25, no. 4, July 1989, pp. 3064-3066.
[2] K.Hameyer, R.Belmans, R.De Weerdt, E.Tuinman: "FEM analysis of steady state behavior of squirrel cage induction motors compared with measurements", IEEE Trans. on Magn., no.2, vol.33, pp.2093-2096.
[3] D. Lederer, A. Kost, "Modelling of Nonlinear Material using a Complex Effective Reluctivity," IEEE Trans. on Magn. no.5, vol.34, Sept. 1998, pp.3060-3063.
[4] S.Yamada, K.Bessho, J.Lu, "Harmonic Balance Finite Element Method Applied to Nonlinear AC Magnetic Analysis," IEEE Trans. on Magn., vol. 25, no. 4, July 1989, pp. 2971-2973.
[5] J.Driesen, G.Deliége, T.Van Craenenbroeck, K.Hameyer, "Implementation of the harmonic balance FEM method for large-scale saturated electromagnetic devices", Electrosoft ' 99 conf., Sevilla, Spain, 17-19.05.' 99, pp.75-84.